Influence of a porous corrosion product layer on the corrosion phenomenon of carbon steel pipelines

Maalek Mohamed-Saïd[1], Patrick Namy[1]
[1]SIMTEC, 155 Cours Berriat, 38000 Grenoble, France

Abstract: In this paper the influence of a porous Corrosion Product Layer (CPL) on the internal corrosion of carbon steels pipeline in a de-aerated and carbonated medium is studied. Based on the literature, a 1D numerical model taking into account a porous CPL is built with COMSOL Multiphysics®.

Results show that the diffusion of species through the CPL and a bilayer structure of the CPL influence in large extend the corrosion process. Favorable conditions for further corrosion product precipitation are highlighted indicating that the precipitation process should be included for complete understanding of the CPL's protectivity.

Keywords: Uniform corrosion, Corrosion Product Layer, Diffusion, CO_2 Corrosion.

1. Introduction

Assessing the severity of the internal corrosion of structures is of paramount importance in the oil & gas industry. Modelling and simulation of this process proved to be key techniques to understand its mechanism and the main factors influencing its severity [**1-4**].

Considerable effort has been deployed to implement an adequate electrochemical process of the corrosion phenomenon [**5-12**]. However, to our knowledge, except [**13-15**], the influence of transport phenomenon through a porous corrosion product layer (CPL) on the corrosion rate has not been studied extensively yet. The transport phenomenon can influence the corrosion rate significantly by either limiting or accelerating the cathodic contribution. In this paper the general corrosion of a carbon steel under a porous CPL of siderite is studied and the influence of the transport phenomenon is examined using COMSOL Multiphysics®. A diagram of the process is presented in **Figure 1**.

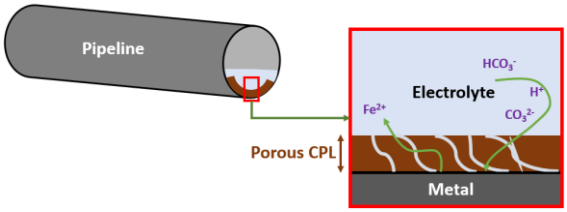

Figure 1: Schematic representation of a porous corrosion product layer (CPL) formed on a carbon steel pipeline

In this paper, it is assumed that the CPL is composed solely of siderite ($FeCO_{3(s)}$) and that the very nature of the CPL does not play a role on the corrosion rate. A 1D numerical model studying general corrosion under a porous CPL and accounting for chemical evolution in the electrolyte is presented. The electrochemical processes and the corresponding kinetics data implemented are the same as detailed in Nesic *et al.* [**3, 5-6**]. Then, it is shown that the CPL's porosity and effective diffusion through the CPL play an important role on the evolution of the chemistry near to the metal surface and consequently on the corrosion rate of the carbon steel.

This model constitutes a first step and can be used for further development to assess the effects of either, a competitive diffusion trough a CPL or a conductive CPL, on the corrosion phenomenon. In fact, the transport phenomenon can play a fundamental role beyond the simple fact of limiting or accelerating the cathodic contribution. It is suggested that the transport from and/or to the steel bare to and/or from the bulk solution could greatly influence the

protectiveness of a corrosion product layer and consequently the corrosion rate of carbon steels [**13-15**]. Finally, the electrochemical behavior of the CPL [**16-17**] could also increase the delocalization of the cathodic reaction all along the CPL leading to a significant increase of the corrosion rate [**17**]. Although the necessary basis to the development of this last point is presented and built in this study, this last point will not be developed in this paper.

2. Theory

The model developed in this paper is based on the transport and reactive phenomena. For a non-porous and non-convective media, the Nernst-Planck equation accounting for the diffusion and migration transport phenomena is given by **Eq-1**:

$$\frac{\partial c_i}{\partial t} + \nabla.(\sum_i(-D_i\nabla c_i - z_i u_i F c_i \nabla\varphi_L)) = R_i \quad \textbf{(Eq-1)}$$

with:

- D_i : the diffusion coefficient ($m^2.s^{-1}$);
- z_i : the number of charge;
- u_i : the mobility given by $D_i/(R.T)$, with R the gas constant (8,314 $J.mol^{-1}.K^{-1}$) and T the temperature (25°C);
- F : Faraday constant (96485 $C.mol^{-1}$) ;
- c_i : concentration ($mol.m^{-3}$);
- R_i : reaction rate, considered at equilibrium ($mol.m^{-3}.s^{-1}$);
- φ_L : the electrostatic potential of the solution (V);

The electrostatic potential (φ_L) satisfies the Poisson equation (**Eq-2**):

$$\nabla^2\varphi_L = -\frac{F}{e}\sum_i z_i c_i \quad \textbf{(Eq-2)}$$

where e is the dielectric permittivity of the medium ($7.08.10^{-11}$ $F.m^{-1}$ at 25°C). It is worth noting that the ratio F/e is sufficiently large to assume the electroneutrality condition given by **Eq-3**:

$$\sum_i z_i c_i = 0 \quad \textbf{(Eq-3)}$$

Thus, the system given by **Eq-1** to **Eq-3**, describes the conservation of the species in an electrically neutral medium.

Electrochemical process

The corrosion of metal implies an electrochemical reaction, namely the oxidation and the reduction. The first is called the anodic process (**Eq-4**) and the second the cathodic process (**Eq-5 to Eq-7**) corresponding respectively to the dissolution of the metal and the reduction on the metal surface of species characterizing a de-aerated and carbonated medium.

Iron oxidation:

$$Fe_{(s)} \rightarrow Fe^{2+} + 2e^- \quad \textbf{(Eq-4)}$$

Water reduction:

$$2H_2O + 2e^- \rightarrow H_2 + 2OH^- \quad \textbf{(Eq-5)}$$

Proton reduction:

$$2H^+ + 2e^- \rightarrow H_2 \quad \textbf{(Eq-6)}$$

Carbonic acid reduction:

$$2H_2CO_3 + 2e^- \rightarrow H_2 + 2HCO_3^- \quad \textbf{(Eq-7)}$$

The electrochemical process considered here has been largely discussed in the domain of oil & gas production facilities [**5-12**]. This electrochemical process is expressed as current density accounted positively for the anodic process and negatively for the cathodic process. These current densities depend on the mass transport limitations and charge transfer resistances.

Table 1 and **Table 2** give the electrochemical process considered in this paper and the corresponding current density. All the kinetics data related to the electrochemical process are taken from Nesic *et al.* [**3**]. Though the validity of the electrochemical process nor the associated current density are discussed in the paper herein since it is not the objective of this study, it may be noted that there is no consensus on the exact electrochemical mechanism to be adopted. Interested readers can refer to [**18-23**] in order to figure out the discussions being still open concerning the electrochemical process.

Table 1: Electrochemical process and current density. With $\eta = \varphi_m - \varphi_L - E_{iref}$. φ_m corresponds to the metal potential and ε_L is the porosity of the CPL.

	Current density	Tafel slope	Reference /ENH
Eq-4	$ia_{Fe} = (\varepsilon_L).ia^0_{Fe}.10^{\frac{\eta}{\beta_a}}$	$\beta_a = 40\ mV$	$E_{refFe} = 447\ mV$

Eq-5	$ic_{H_2CO_3} = -(\varepsilon_L).ic^0_{H_2CO_3}.10^{-\frac{\eta}{\beta_{cH_2CO_3}}}$	$\beta_{cH_2CO_3} = 120\ mV$	$E_{refH_2CO_3} = 381\ mV$
Eq-6	$ic_{H_2} = -(\varepsilon_L).ic^0_{H_2}.10^{-\frac{\eta}{\beta_{cH_2}}}$	$\beta_{cH_2} = 118\ mV$	$E_{refH_2} = 0$
Eq-7	$ic_{H_2O} = -(\varepsilon_L).ic^0_{H_2O}.10^{-\frac{\eta}{\beta_{cH_2O}}}$	$\beta_{cH_2O} = 118\ mV$	$E_{refH_2O} = 827\ mV$

Table 2: Apparent current density given at T=25°C.

Expression of the apparent current density	Concentration (mol.m^{-3})
$ia^0_{Fe} = 1\ A.m^{-2}.\left(\frac{c_H}{C_{H_{ref1}}}\right)^{a_1}.\left(\frac{c_{CO_2}}{C_{CO_{2ref}}}\right)^{a_2}$ $a_1 = \begin{cases}1, & P_{CO2} < 1\ bar\\ 0, & P_{CO2} \geq 1\ bar\end{cases}$ $a_2 = \begin{cases}2, & pH \leq 4\\ 1, & pH \in]4;5]\\ 0, & pH > 5\end{cases}$	$C_{H_{ref1}} = 0{,}1$ $C_{CO_{2ref}} = 36{,}6$
$ic^0_{H_2CO_3} = 0{,}06\ A.m^{-2}.\left(\frac{c_H}{C_{H_{ref2}}}\right)^{-0,5}.\left(\frac{c_{H_2CO_3}}{C_{H_2CO_{3ref}}}\right)$	$C_{H_{ref2}} = 0.01$ $C_{H_2CO_{3ref}} = 0{,}1$
$ic^0_{H_2} = 3.10^{-5}\ A.m^{-2}.\left(\frac{c_H}{C_{H_{ref3}}}\right)^{0,5}$	$C_{H_{ref3}} = 0{,}1$
$ic^0_{H_2O} = 3.10^{-5}\ A.m^{-2}$	–

Finally, the unknown electrical potential at the metal surface, called corrosion potential or rest potential, is obtained from the charge balance equation at the metal surface: $\sum i_a = |\sum i_c|$.

Equilibrium reaction

In addition to the electrochemical reaction, species created and/or consumed at the metal surface and those present at the initial stage will evolve within the solution. It is considered that all species will evolve at equilibrium. Four equilibriums are considered:

Autoprotolysis of Water: $K_w = 10^{-14}$

$$H_2O = H^+ + OH^- \qquad \textbf{(Eq-8)}$$

Hydration of CO_2: $K_{CO2} = 2{,}580.10^{-3}$

$$CO_2 + H_2O = H_2CO_3 \qquad \textbf{(Eq-9)}$$

First dissociation of H_2CO_3: $K_{H2CO3} = 1{,}251.10^{-4}$

$$H_2CO_3 = HCO_3^- + H^+ \qquad \textbf{(Eq-10)}$$

Second dissociation of H_2CO_3: $K_{HCO3} = 1{,}382.10^{-10}$

$$HCO_3^- = CO_3^{2-} + H^+ \qquad \textbf{(Eq-11)}$$

The thermodynamic data are those used by *Nesic et al.* [**3, 5-6**].

Transport through porous layer

The scope of this paper is not the study of the electrochemical process but rather to examine the transport of species through a porous corrosion product layer and its effect on the corrosion process.

The transport of species through a porous corrosion layer (CPL) will affect the corrosion process because of two phenomena; the covering of the metal surface by the CPL and the limitation of the transport of the species through the CPL.

A porous corrosion product layer of thickness (L) and porosity (ε_L) is considered. Later, the porosity of the CPL will be addressed in a parametric study.

Thus, in this case, for a porous medium, the Nernst-Planck equation, within the CPL will be given by :

$$\frac{\partial(\varepsilon_L.c_i)}{\partial t} + \nabla.\left(\sum_i\left(-D_{i,eff}\nabla c_i - z_i u_{i,eff} F c_i \nabla\varphi_L\right)\right) = R_i.\varepsilon_L \qquad \textbf{(Eq-12)}$$

where the effective diffusion ($D_{i,eff}$) follows the well-known Bruggeman correlation for the transport phenomena in porous medium:

- $D_{i,eff} = D_i.\varepsilon_L^{1,5}$;
- $u_{i,eff} = \frac{D_{i,eff}}{R.T}$.

Within the CPL the diffusion and the migration of chemical species are affected by the porosity of the layer expressing the less and/or more tortuous path from and to the metal surface. In **Table 3,** the diffusion coefficient of each chemical species considered in this work are presented.

Table 3: Diffusion coefficient of species considered in the present study

Species	Diffusion coefficient 10^{-9} (m^2.s^{-1})
Fe^{2+}	0,72
H^+	9,30
OH^-	5,26
CO_2	1,96
H_2CO_3	2,00
HCO_3^-	1,10
CO_3^{2-}	0,92

Na^+	1,33
Cl^-	2,03

In equation (Eq-12), the reaction terms, R_i, takes into account the reduction of the volume and the electrochemical process will be altered to reflect the effective area being corroded. This will be detailed in section 4.

3. Governing Equations / Numerical Model

In this section, initial and boundary conditions are detailed and the use of COMSOL Multiphysics® is described in order to facilitate an eventual development for the interested readers.

Numerical Model

A 1D numerical model is built in which the metal surface is represented by a node and the electrolyte is represented by an interval as large as the diffusion layer (δ) as depicted in **Figure 2**.

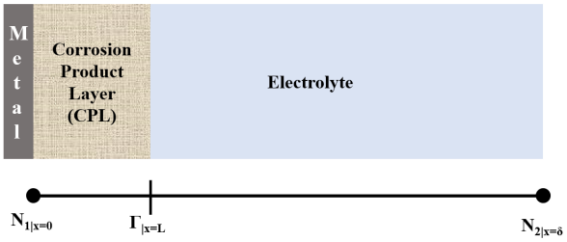

Figure 2: Schematic representation of the simulated domain.

At the metal surface ($\mathbf{N_{1|x=0}}$) the following boundary conditions are set:

- zero flux for non-electroactive species;
- fluxes depending on the current density for electroactive species, $N_i=f(i_{a,c})$:
  - $N_{Fe^{2+}} = \frac{ia_{Fe}}{2*F}$;
  - $N_{H^+} = -\frac{|ic_{H_2}|}{F}$;
  - $N_{H_2CO_3} = -\frac{|ic_{H_2CO_3}|}{F}$;
  - $N_{HCO_3} = \frac{|ic_{H_2CO_3}|}{F}$;
  - $N_{OH^-} = \frac{|ic_{H_2O}|}{F}$.

At the diffusion boundary layer ($\mathbf{N_{2|x=\delta}}$) a condition of concentration modelling an open boundary is fixed.

Finally, the initial composition of the medium, given hereafter in **Table 4**, is a calculated composition verifying the equilibrium specified in **Eq-8** to **Eq-11** for pH=5. The concentration of Na^+ is calculated in order to respect the electroneutrality of the solution.

Table 4: Initial composition of the medium

Species	Concentration ($mol.m^{-3}$)
Na^+	$-\sum z_i.c_i,\ i \neq Na^+$
Cl^-	10
Fe^{2+}	$1{,}79.10^{-2}$
OH^-	9.10^{-7}
H^+	10^{-2}
CO_2	33,3
H_2CO_3	$8{,}6.10^{-2}$
HCO_3^-	2,34
CO_3^{2-}	$3{,}17.10^{-5}$

Numerical tool

The Corrosion Module of COMSOL Multiphysics® is used to solve a PDE system. For the physical properties of the CPL, a separator generally used in batteries is used. As for the metal surface, an electrode surface is defined under which the four electrochemical reactions presented in section 2 are defined.

4. Results / Discussion

Influence of the porosity of the CPL

Firstly, five different porosities are assessed: 0,8; 0,3; 0,1; and 0,01.

In **Figure 3** it is shown how the porosity of the CPL affects the corrosion rate by covering the metal surface. Obviously, a dense layer (low porosity) involves high surface coverage and consequently a low corrosion rate.

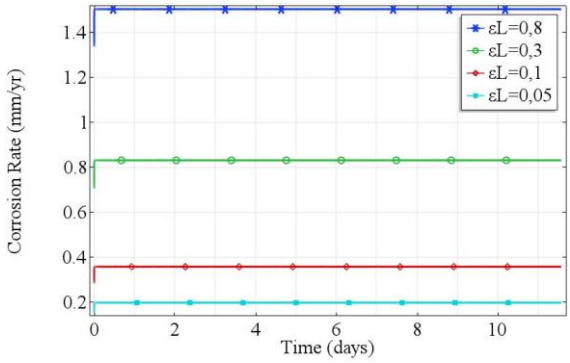

Figure 3: Evolution of the corrosion rate for four CPL's porosities.

As early mentioned, the study presented in this paper is focused on the transport phenomena and it is worth noting that a denser layer limits the transport within the CPL and, as depicted in **Figure 4**, the pH increases significantly. In other words, pH increase is due to the limitation of the bicarbonate diffusion through the CPL.

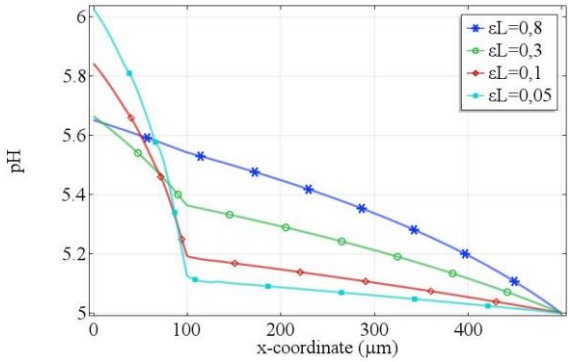

Figure 4: pH distribution for four CPL's porosities

In this case, one may obtain a high saturation level of the siderite. The saturation level is a thermodynamic indication of either or not the siderite could precipitate. In this case, as shown in **Figure 5**, the saturation level is lead by the distribution of the pH. Thus, the denser the layer the more protective it is for at least two reasons:

- high metal surface coverage;
- limitation of the transport leading to high pH, and consequently to conditions ensuring the precipitation of corrosion products (the precipitation phenomena is not taken into account in this paper).

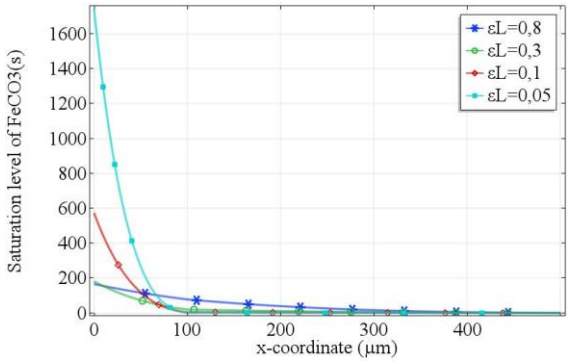

Figure 5: Distribution of the saturation level of the siderite for four CPL's porosities

The question to be posed is which of these two effects influences most efficiently the corrosion process: the covering effect or the transport limitation.

Influence of the bilayer structure of the CPL

The objective of this last study is to figure out which of the covering effect or the transport limitation influences most the corrosion process. To do so, a bilayer structure is assumed, here an internal layer and an external layer are considered, as schematically represented in **Figure 6**.

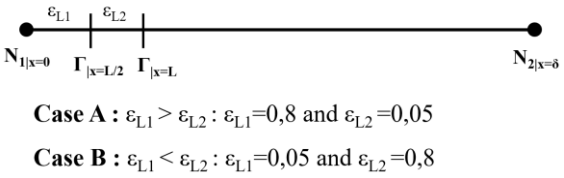

Case A : $\varepsilon_{L1} > \varepsilon_{L2}$: ε_{L1}=0,8 and ε_{L2}=0,05

Case B : $\varepsilon_{L1} < \varepsilon_{L2}$: ε_{L1}=0,05 and ε_{L2}=0,8

Figure 6: Schematic representation the CPL's bilayer structure considered.

Two cases are considered, in the first case (Case A) the internal layer is less dense than the external one, and inversely, in the second case (Case B) the internal layer is denser than the external part.

In **Figure 7** it can be seen that the porosity of the internal layer controls the corrosion rate. It is also important to highlight that in the first case (Case A) one can notice that the corrosion rate decreases from 1,5 mm/yr (**Figure 3**) to 1,2 mm/yr (**Figure 7**) which means the transport phenomenon has a marginal effect on the corrosion rate with respect to the effect of the metal covering as highlighted in the second case (Case B). Readers can refer to [**24**] for further discussions on these types of configuration.

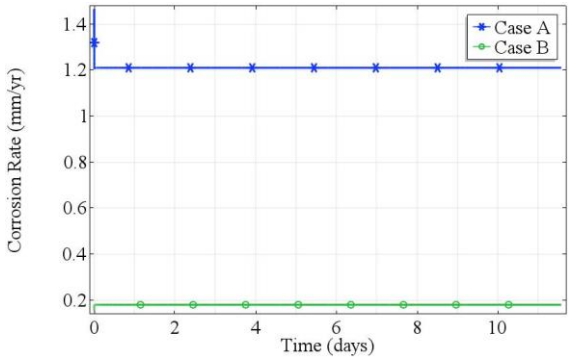

Figure 7: Evolution of the corrosion rate

When it comes to the chemical evolution of the medium, this marginal effect is no longer true. In case B, where a denser layer at the external part is considered, the pH (**Figure 8**) and the saturation level (**Figure 9**) increase significantly indicating more favorable conditions for the corrosion products to precipitate.

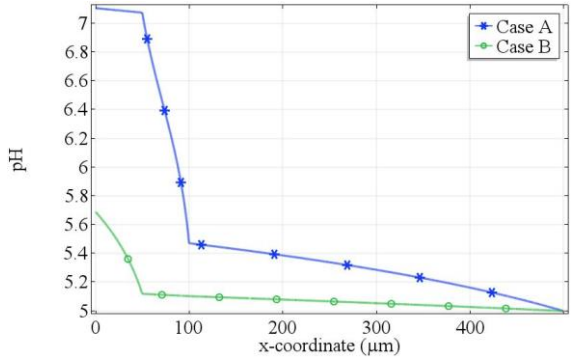

Figure 8: Distribution of the pH.

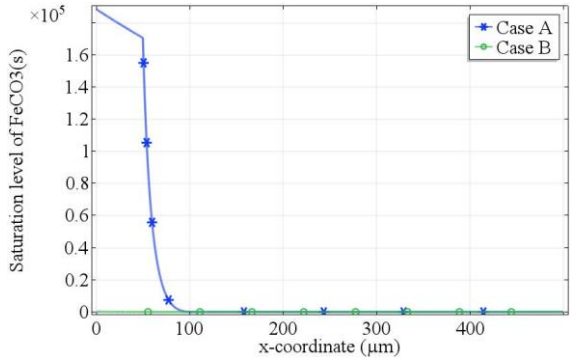

Figure 9: Distribution of the saturation level of the siderite.

As already mentioned, the precipitation of the corrosion product is not considered; however it is obvious that if the precipitation phenomenon was considered, results from Case B would lead to high precipitation rate and perhaps to a more protective CPL. This point will be addressed in another following paper where the precipitation process will be considered.

5. Conclusions

In this paper, a 1D numerical model designed to study the effect of a porous corrosion product layer on the corrosion rate in a de-aerated and carbonated medium was presented with an emphasis on the effect of the transport phenomenon on the corrosion process. It was found that:

- the corrosion rate depends largely on the porosity of the internal part of the CPL that covers the metal surface;
- an external dense layer affects mainly the chemical composition and thus the corrosion process by limiting the transport at the external part.

The first point corresponds to an obvious result since the CPL covers the active metal surface, thus the corrosion rate decreases. The second point indicates, from a thermodynamic point of view, that the chemical composition would allow the precipitation of a dense corrosion product.

However, it is quite early at this stage to conclude on this point as the precipitation of the corrosion product layer could introduce other complexities that are not supported by this study. Indeed, the saturation level of the siderite indicates whether precipitation is thermodynamically possible or not, but do not give any indication on how fast precipitation can occur and how the precipitation kinetics can influence the corrosion process. This last point will be addressed in a future publication.

6. References

1. C. De Waard, D.E. Milliams, “Carbonic acid corrosion of steel”, Corrosion, 31, (1975).
2. C. De Waard, D.E. Milliams, “Predictive model for CO_2 corrosion engineering in wet natural gas pipelines”, Corrosion, 47, 976-985, (1991).
3. M. Nordsveen, S. Nesic, R. Nyborg, A. Stangeland, “A mechanistic model for carbon dioxide corrosion of mild steel in the presence of protective iron carbonate films part 1: theory and verification”. Corrosion 59, 443-456, (2003).
4. S. Nesic, K.L.J. Lee, “A mechanistic model for carbon dioxide corrosion of mild steel in the presence of protective iron carbonate

films-part 3: film growth model", Corrosion, 59, 616-628, (2003).
5. S. Nesic, J.L. Crolet, D. M. Drazic "Electrochemical properties of iron dissolution in the presence of CO_2 – Basics revisited", Nace Corrosion papier N°3, (1996).
6. S. Nesic, J. Postlethwaite, S. Olsen, "An Electrochemical Model for Prediction of Corrosion of Mild Steel in Aqueous Carbon Dioxide Solutions" Corrosion, 52, 280-294, (1996).
7. G. Schmitt, B. Rothmann, "Corrosion of unalloyed and low alloyed steels in carbonic acid solutions", Werkstoffe und Korrosion, 29, 237-245, (1978).
8. L. G. S. Gray, B. G. Anderson, M. J. Danysh, P. G. Tremaine, "Mechanisms of Carbon Steel Corrosion in Brines Containing Dissolved Carbon Dioxide at pH 4", Corrosion Nace Paper N°464, (1989).
9. L.G.S. Gray, B.G. Anderson, M.J. Danysh, P.G. Tremaine, "Effect of pH and temperature on the mechanism of carbon steel corrosion by aqueous carbon dioxide" Corrosion Nace, Papier N°40, (1990).
10. E. Remita, B. Tribollet, E. Sutter, V. Vivier, F. Ropital, J. Kittel, "Hydrogen evolution in aqueous solutions containing dissolved CO_2: Quantitative contribution of the buffering effect", Corrosion science, 50, 1433-1440, (2008).
11. T. Tran, B. Brown, S. Nesic, "Corrosion of Mild Steel in an Aqueous CO_2 Environment – Basic Electrochemical Mechanisms Revisited", Corrosion Nace, Papier N° 5671, (2015).
12. A. Kahyarian, M. Singer, S. Nesic, "Modeling of uniform CO_2 corrosion of mild steel in gas transportation systems: A review", Journal of Natural Gas Science and Engineering, 29, 530-549, (2016).
13. J-L. Crolet, "Mécanisme de la corrosion uniforme sous dépôt de corrosion", (1988).
14. J. L. Crolet, "Mechanisms of uniform corrosion under corrosion deposits", Journal of Materials Science, 28, 2589-2606, (1993).
15. J. L. Crolet, "Protectiveness of Corrosion Layers", Modelling Aqueous Corrosion, K. R. Trethewey and P. R. Roberge, Éd. Springer Netherlands, 1-28, (1994).
16. J. L. Crolet, N. Thevenot, S. Nesic, "Role of Conductive Corrosion Products in the Protectiveness of Corrosion Layers", Corrosion, 54,194-203, (1998).
17. M. Mohamed-Saïd, B. Vuillemin, R. Oltra, L. Trenty and D. Crusset "One-dimensional porous electrode model for predicting the corrosion rate under a conductive corrosion product layer", Journal of The Electrochemical Society, (2017).
18. M. Bonis, "Recherche des mécanismes de la corrosion de l'acier par le gaz carbonique dans les installations de production pétrolière", Thèse, INSA de Lyon, (1982).
19. S. Nesic, J.L. Crolet, D. M. Drazic "Electrochemical properties of iron dissolution in the presence of CO_2 – Basics revisited", Nace Corrosion papier N°3, (1996).
20. A. Dugstad, "Fundamental Aspects of CO_2 Metal Loss Corrosion, Part I: Mechanism", Corrosion NACE, Papier N°5826, (2015).
21. S. Nesic, "Key Issues Related to Modelling of Internal Corrosion of Oil and Gas Pipelines – A Review" Corrosion Science, 49, 4308-4338, (2007).
22. A. Kahyarian, M. Singer and S. Nesic, "Modeling of uniform CO_2 corrosion of mild steel in gas transportation systems: A review", Journal of Natural Gas Science and Engineering, 29, 530-549, (2016).
23. T. Tran, B. Brown, S. Nesic, "Corrosion of Mild Steel in an Aqueous CO_2 Environment – Basic Electrochemical Mechanisms Revisited" NACE Corrosion/2015 Conference, N°5671, (2015).
24. M. Mohamed-Saïd, "Modélisation du rôle des produits de corrosion sur l'évolution de la vitesse de corrosion des aciers au carbone en milieu désaéré et carbonaté", Thèse Univ. de Bourgogne Franche-Comté, (2018).